Proceedings of the Twenty-second (2012) International Offshore and Polar Engineering Conference
Rhodes, Greece, June 17–22, 2012

ISBN 978-1-880653-94–4 (Set); ISSN 1098-6189 (Set)

www.isope.org

Realistic Moving Ice Loads and Ship Structural Response

Bruce W.T. Quinton and Claude G. Daley
Faculty of Engineering, Memorial University of Newfoundland
St. John's, Newfoundland, Canada

Robert E. Gagnon
Institute for Ocean Technology - National Research Council of Canada
St. John's, Newfoundland, Canada

ABSTRACT

Prior work by the authors has shown that moving ice loads incite a significantly different structural response in steel grillage structures than do stationary ice loads. The work was based on a validated explicit numerical model of a steel grillage. The main drawback was that the ice load model was largely unrealistic in terms of the distributed pressure and ice motions. The present work employs two realistic ice load models: a dynamic 4D pressure model, and a validated "crushable foam" ice model. Results using these realistic ice load models lend credence to previous findings and enable more realistic modeling of the whole ice-ship impact scenario.

KEY WORDS: realistic; moving; ice; damage; 4D; pressure; dynamic.

INTRODUCTION

The accepted standard for the design and analysis of ice-classed ship structures is to assume a stationary load resulting from a glancing impact with an ice edge (IACS URI I2.3.1). Since not all ice loads are stationary glancing impacts, this raises several important questions: *Are structural designs/analyses based on stationary loads valid when the loads are not stationary? Are the structural failure mechanisms associated with moving ice loads the same as those for stationary loads? Is it valid to assume the design case for ice-classed structures is a stationary load?*

Previous works by the authors have identified the basic structural response mechanisms of a grillage to moving loads (Quinton 2009; Kendrick, Daley, and Quinton 2009; Quinton, Daley, and Gagnon 2010). A moving load consists of two coupled parts: the component normal to the grillage's plating, and the corresponding tangential component. This previous work endeavored to uncouple these load components by using a simple loading method that applied them sequentially to the grillage structure (i.e. the grillage was loaded normal to the plate, then the load was translated laterally along the plate). This simple loading method allowed the structural response of the grillage to be observed for each load component; independent of the other.

This work was carried out using an explicit nonlinear finite element model. This model was based on – and validated against – full-scale experiments involving two identical steel grillages that were designed to check the IACS polar class structural limit state formulations (Daley and Hermanski 2008a; 2008b). Each experimental grillage (the yellow structure shown in Figure 1) was a 6.756 m long by 1.5 m wide full-scale representation of the side shell of a PC6 IACS ice-strengthened ship (IACS 2007).

Figure 1. Full-scale steel grillage experimental setup.

The "simple load method" discussed above was implemented in the numerical model through the use of a rigid indenter in contact with a grillage model.

While the loading method described above was beneficial in identifying the basic structural response mechanisms of a grillage to a moving load, it has the severe drawback of being generally unrealistic when compared with existing knowledge of real ice loads in terms of its uncoupled motions as well as its spatial and temporal pressure distribution.

This present work focuses on the analysis of the same numerical

grillage model, for two separate "realistic" moving ice load methods: the crushable foam method and the 4D ice pressure method. The term "realistic" is used because these two methods do not decouple the normal and tangential components of the moving loads, and they develop ice pressure distributions in accordance with actual laboratory and field observations. In fact, the 4D ice pressure method can be used to apply actual laboratory and field observations directly to a numeric structural model.

This paper begins by highlighting the grillage finite element model and the structural response mechanisms observed during previous investigations for the simple loading method. It then presents the two realistic ice load methods, followed by a description of the new simulations and their results. Ultimately, this work shows that the same basic structural response mechanisms that were observed for the simple load method (i.e. uncoupled, uniform pressure moving loads) are present for the realistic moving ice load methods.

BACKGROUND

This section briefly describes the numerical model and the structural behaviours observed for the simple load method discussed above.

Numerical Model Details

The numerical model employed in these and the prior works discussed above is an explicit non-linear finite element model (Quinton 2009; Quinton, Daley, and Gagnon 2010) generated using the popular and proven LS-DYNA code by Livermore Software Technology Corp.

The geometry consists entirely of planar areas (see Figure 2) meshed with standard 4-node Belytschko-Tsay shell elements with five through-thickness integration points. The Belytschko-Tsay element formulation treats bending, membrane and shell thickness changes, and employs reduced integration, includes transverse shear and has built in hourglass control.

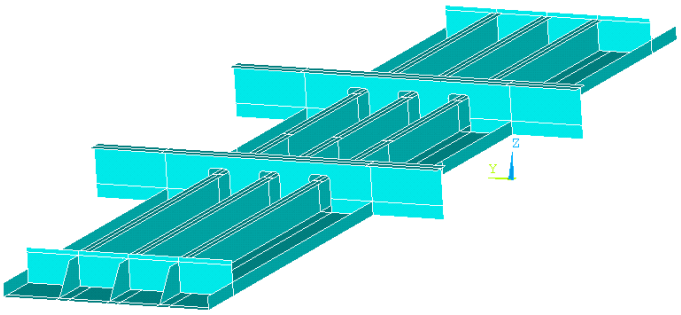

Figure 2. Numerical model grillage geometry.

A mesh convergence study for this model was conducted, which showed convergence for a mesh density of 4279 elements/m^2; resulting in a total number of shell elements of 80,874 (mesh shown in Figure 3).

A bilinear isotropic elasto-plastic material model was used for all shell elements. The inputs (see Table 1) for this material model were derived from the results of physical material tensile tests on steel specimens taken from the physical grillage used in the experiments mentioned above. Paik's "knock-down factor approach" (Paik 2007) was used to resolve the bilinear material model inputs from the engineering stress-strain results of the tensile tests.

The bolt patterns used to attach the large grillage structure to the test frame during the physical experiments were such that rotations and displacements in all degrees of freedom were fixed. Nodes in the numerical model that were coincident with the location of these bolts were constrained in all rotational and translational degrees of freedom.

Table 1. Large Grillage material model parameters.

Density kg/m^3	Young's Modulus GPa	Poisson's Ratio	Yield Stress MPa	Tangent Modulus MPa	Cowper Symonds C 1/s	Cowper Symonds p
7850	200	0.3	350	1000	40.4	5

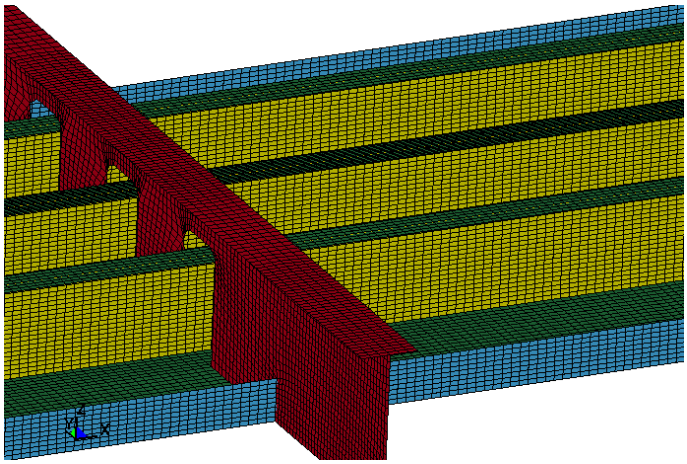

Figure 3. Finite element mesh.

Grillage Behavior for Simplified Moving Loads

In the context of comparing stationary versus moving loads, it was found that the application of stationary loads to the grillage (whether or not they caused any permanent plastic damage) incited a relatively symmetric structural response; where symmetry was permitted by the structure's geometry. That is, all structure radially adjacent to the point of application of a stationary load participated relatively equally in response to that load. This response symmetry is evident in Figure 4; which shows various types of structural reactions to a 2 cm stationary indentation into the grillage's plating.

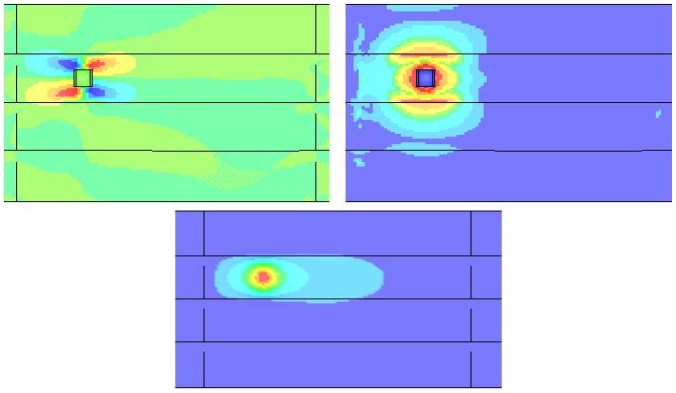

Figure 4. Example response to a stationary load: *Mxy* moment distribution (top left), max in plane stress (top right), residual plate displacement (bottom). Note: the indenter is shown as a green or blue square in the top left and right plots respectively.

Moving loads causing an elastic structural response in the grillage (i.e. loads that caused no permanent structural damage) showed no new structural mechanisms; over and above those already present during the stationary load phase. The same reaction mechanisms, shown in Figure

4, were simply translated along with the load, without appreciable change in their magnitude or shape.

Moving loads that caused permanent plastic structural damage were an entirely different matter, as significant changes in the structural response mechanisms were evident. Instead of responding symmetrically to the load (as was the case for stationary loads), a distinct asymmetric response was observed. That is, the structure on the trailing side of the moving load did not appear to be contributing significantly to the overall structural response. Invariably, and regardless of the loading scenario (e.g. load moving along on a frame, moving on the plate between frames, crossing frames, etc...) a distinct and immediate drop in structural load capacity of the grillage was observed upon commencement of the moving loads. In addition, it was observed that subsequent to the initial drop in load capacity, as a moving load approached a section of the structure that was structurally stiffer than its current location, the level of damage caused by the moving load would increase with decreasing proximity to the stiffer section. For example, if a load was moving along a frame towards a stringer, the frame would begin to buckle (or if already buckled, the amount of buckling would increase). To further illustrate the difference between moving and stationary loads, consider that at a known location along the central frame near a stringer, a stationary indentation of approximately 7 [cm] was required before the frame began to buckle. At the same location, the frame buckled for a 2 [cm] moving load.

Figure 5 shows example structural reaction curves that illustrate these decreases in structural capacity. The curves drawn in red "X" and blue "-" points show the grillage's structural reaction to 2 and 5 cm (respectively) moving indentations acting on plating only (i.e. between frames) and moving laterally over the distance between the stringers. The load at 0 [m] lateral displacement is not zero, as this point represents the location of the stationary portion of the uncoupled moving load (i.e. before any lateral motion of the load along the plate, the stationary indentation portion of the load takes place). Note that as soon as the load begins to move laterally, there is a significant drop in the structural reaction force, even though the displacement of the indenter into the plating has not changed. The curve drawn in green "+" points shows the grillage's reaction force to an 2 cm indentation moving along the central frame and across the two stringers. The location of the stringers are shown by the large increase in reaction force at a location of about 1.5 and 3.5 [m] lateral displacement. Aside from the initial capacity drop at 0 [m] lateral displacement, there is an additional, subsequent drop in load capacity as the load approaches the stringers. This is caused by the onset of frame buckling as the moving indenter nears the much stiffer stringer.

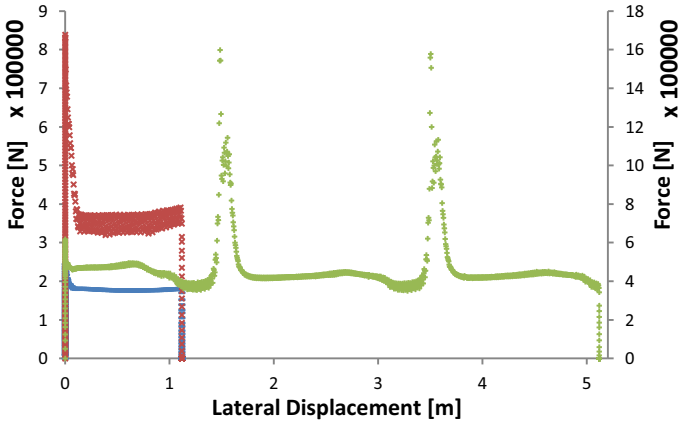

Figure 5. Example reaction force vs. lateral load displacement curves for various load scenarios causing permanent structural damage.

Analysis of all the load cases studied in prior works by the authors has shown that – because the structure on the trailing side of the moving load was plastically damaged – its ability to exert a reaction force on the indenter via bending and through-thickness shear was compromised; and the reaction force was provided primarily by the undeformed structure on the leading side of the moving load.

REALISTIC ICE LOAD MODELS

As mentioned above, "realistic" ice load models incorporate coupled normal and tangential motions with respect to the ship's plating, and provide pressure distributions representative of measured field and laboratory ice load data. Two realistic ice load methods were employed for this paper: the crushable-foam method, and a novel 4D ice pressure method.

Crushable-foam Ice Load Model

The crushable-foam ice load method was developed by Gagnon (2007) in order to model impacts between ships and glacial ice. It was implemented in LS-DYNA (Livermore Software Technology Corp.) and requires that the ice be modeled using solid finite elements employing a crushable-foam material model. Ice loads are transmitted to a separate finite element mesh (e.g. the grillage structure used in this paper) via a contact algorithm. The material model inputs were derived by Gagnon based on measured field (Gagnon, Cumming, Ritch, Browne, Johnston, Frederking, McKenna, and Ralph 2008) and laboratory experiments involving ice tank model tests and ice crushing experiments (Gagnon 2004a; 2004b; 2004c).

For the purposes of this paper, the crushable-foam ice model was implemented in the form of a conical ice sample (0.5 m radius with a 30° elevation angle) constrained by an aluminum holder that is attached to a rigid backing plate (see Figure 6). The purpose of the backing plate is to provide additional mass to the ice-holder in order to simulate much more massive pieces of glacial ice. The mass of the rigid backing plate is varied by controlling the density of the rigid material model.

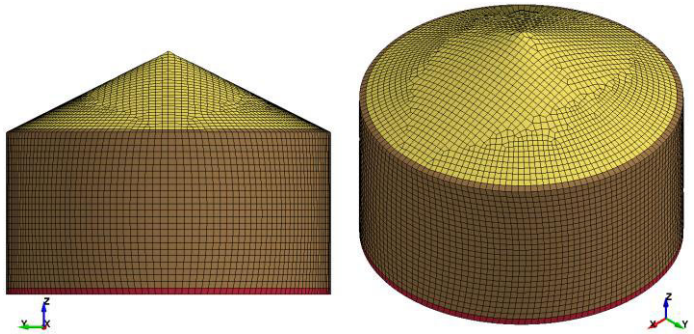

Figure 6. Crushable-foam ice conical ice sample (yellow) in aluminum holder (brown) with rigid backing plate (red).

The model contains 61,350 solid elements. Their size provides a constant mesh density throughout the model and ensures that the element face sizes are approximately equivalent to the size of the shell elements in the grillage model. For the specific details of the crushable foam material model the reader is referred to Gagnon (2007). The aluminum is modeled with the MAT_ELASTIC material model; using a mass density of 2600 kg/m^3, a Young's modulus of 69 GPa, and a Poisson's ratio of 0.35. The backing plate uses the MAT_RIGID material model with variable mass density depending on the mass required for the simulation in question. The other inputs for the rigid material model are inconsequential as the rigid body does not partake in

the contact algorithm used to transfer the load to the grillage (but standard values for steel were used). Motion of the ice holder is not controlled subsequent to prescribing it's an initial velocity; except that its rotations are constrained about all three axes.

4D Ice Pressure Loading Method

The 4D ice pressure loading method is a novel method by the authors that may be used to apply ice pressure loads that vary in both time, and 3-dimensional space. Specifically, the data is in the form of (x, y, P(t)); where P(t) is the magnitude of the pressure at time, t, and x and y pinpoint the location of P(t) on a given surface. This method is general in that the pressure distribution(s) applied may vary in location, size, and shape, and may consist of uniform, distributed, or a collection of discrete pressures (uniform or distributed); each of which may vary in magnitude with time. The generality of the method implies that it may be used to model everything from uniform, stationary, steady pressure loads (as is commonly done using standard finite element techniques), to custom ice pressure load models, to actual field and laboratory pressure data measured in time from a pressure sensor array. In addition, the method allows for refinement of the data resolution through the use of two-dimensional interpolation schemes. For example, given data from 6 x 10 pressure sensor array, the method can refine this to any desired resolution (e.g. 11 x 19, 21 x 37, etc.) using either a nearest-neighbor, bilinear, or cubic interpolation scheme; depending on the desired shape (see Figure 7) of the interpolated data. The authors suggest that cubic interpolation provides pressure shapes in line with those observed in the laboratory; however, when using the method for design purposes, the nearest-neighbor method would provide more conservative results. Figure 7 is an example of how the interpolation works. The original 4D input data (for a single instant in time) is shown in the top left, and the other plots are the outputs of the various interpolation methods, for a given interpolation level.

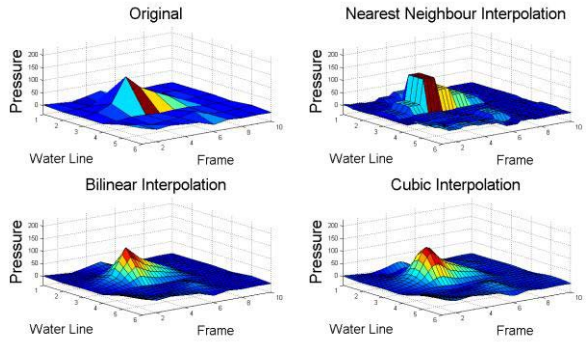

Figure 7. Top left - original 4D pressure data input; Top Right - nearest neighbor interpolation; Bottom Left - bilinear interpolation; Bottom Right - cubic interpolation.

A limitation of the 4D ice pressure method is that the pressure is prescribed in time, without regard for the effects that the reaction of the structure has on the load itself. This is of course, no different than any other contactless loading method.

The 4D ice pressure method was developed using Matlab (The Mathworks, Inc.). A Matlab script reads (x, y, P(t)) data, interpolates it (if desired), and then writes a corresponding LS-DYNA input deck (i.e. kfile).

For the purposes of this investigation, the 4D ice pressure method was used to create a single, smooth ice pressure distribution, similar to the large peak shown in Figure 7. The starting point for the creation of this pressure distribution was the shape of an actual ice pressure wave (recorded from the 1980's Polar Sea field trials (St. John, Daley and Blount 1984)) as it travelled over a 6 x 10 pressure sensing array. This recorded wave was normalized in both pressure and time (see Figure 8) to allow for general application to the grillage numerical model, depending on the load case; as described below.

Figure 8. Normalized pressure vs. time wave.

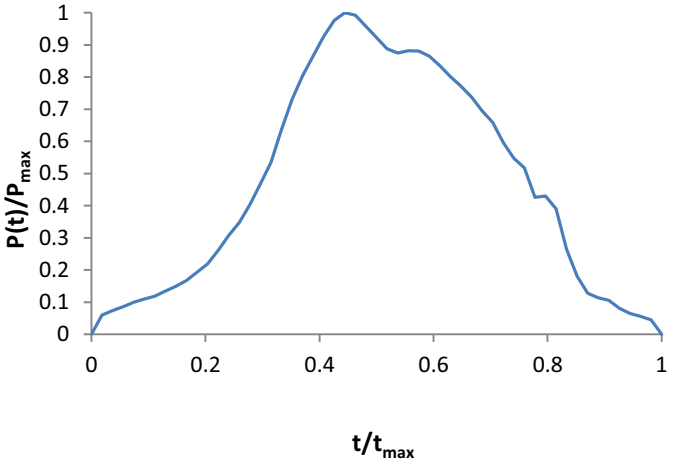

TEST MATRIX

In order to determine the effect of realistic moving ice loads on grillage structures, the structural responses to various applied moving loads were compared with "control" cases in the form of equivalent stationary loads. All loads (moving and stationary) were of sufficient magnitude to cause some level of plastic structural damage. Plastic damage is necessary in the study of the effect of moving loads because, as noted above, it has been previously observed that there is little appreciable difference between moving and stationary loads when the grillage structure remains elastic.

Using the two realistic ice load methods described above, a series of load scenarios were modeled by changing various parameters of the simulation. These parameters were load type, load level, load location with respect to the stringers, and load location with respect to the central frame. Load type is simply whether the load is moving or stationary. Load level was varied by changing the mass of the iceholder (for the crushable foam method tests), or by scaling the pressure distribution (for the 4D ice pressure method). Two levels of load were applied for each method: 25 and 40 tonnes for the crushable foam case, and 15 and 30 MPa (peak) pressures for the 4D ice pressure case. For each of the methods, these loads were applied in the following locations: grillage center below central frame, grillage center between frames, near a stringer on the central frame, and near a stringer between frames. Varying these parameters over two levels resulted in 32 load cases; which are summarized in Table 2.

A few other points should be noted. All loads for the crushable foam method cases were modeled as discrete impact events. All ice holder rotations were constrained, but all translations were not. For all crushable foam moving loads, the ice holder was given a normal (i.e. into the grillage's plating) and a tangential (i.e. along the plating in the direction of the framing) velocity. These velocities were derived by assuming the scenario of an ice strengthened ship transiting growler infested waters at a speed of 10 knots with an angle between hull and the ice of 30°. This resulted in a normal velocity of 2.572 m/s and a tangential velocity of 4.455 m/s. All stationary crushable foam loads were only given a normal velocity of 2.572 m/s.

Table 2. Text Matrix.

Case	Ice Load Model	Load Acting	Level	Location	Type
1	Crushable Foam	On Frame	25 tonne	Central	Moving
2					Stationary
3				Near Stringer	Moving
4					Stationary
5			40 tonne	Central	Moving
6					Stationary
7				Near Stringer	Moving
8					Stationary
9		On Plate	25 tonne	Central	Moving
10					Stationary
11				Near Stringer	Moving
12					Stationary
13			40 tonne	Central	Moving
14					Stationary
15				Near Stringer	Moving
16					Stationary
17	4D Ice Pressure	On Frame	15 MPa (peak)	Central	Moving
18					Stationary
19				Near Stringer	Moving
20					Stationary
21			30 MPa (peak)	Central	Moving
22					Stationary
23				Near Stringer	Moving
24					Stationary
25		On Plate	15 MPa (peak)	Central	Moving
26					Stationary
27				Near Stringer	Moving
28					Stationary
29			30 MPa (peak)	Central	Moving
30					Stationary
31				Near Stringer	Moving
32					Stationary

For the 4D ice pressure load cases, all loads were applied over an area 0.5 [m] x 0.7 [m]; the latter number is two times the frame spacing. All moving loads transited in the tangential direction at 4.455 m/s. All stationary loads were applied as a ramped, stationary, steady pressures. Example moving and stationary 4D ice pressure loads are shown in Figure 9 and Figure 10.

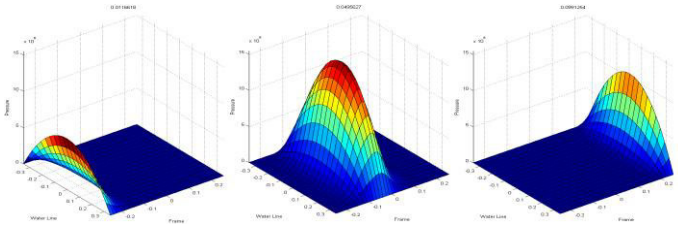

Figure 9. Example 4D moving pressure load.

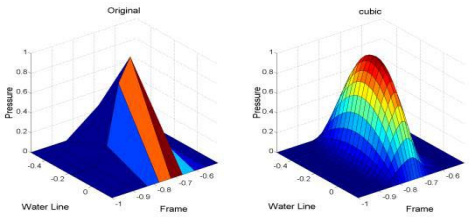

Figure 10. Example 4D stationary pressure load.

STRUCTURAL RESPONSE AND DISCUSSION

The same structural response mechanisms observed in previous works (and discussed above) for the simple load method were present for the realistic ice load methods. That is, structural response was generally symmetric for stationary loads, and asymmetric for moving loads. The damage on the trailing side of the moving load undermined the capacity of that part of the structure to bear the same amount of load as it could if the load was stationary. Thus it becomes the responsibility of the remaining undamaged structure (which is effectively on the leading side of the moving load) to provide an increased response relative to what it would have to provide if the load was stationary.

Given that the results of these load cases support previous findings, rather than presenting an exhaustive list of results for each of the 32 load cases, specific results from illustrative test cases are used to highlight the underlying differences between the grillage's response to realistic moving and stationary ice loads.

Plate Bending

Figure 11 (plan view of grillage) illustrates the effect on the bending response of the grillage's plating to moving loads. This particular case is the 15 MPa (peak) pressure load with the load center located near a stringer and between frames (shown by the black circle for the stationary case, and by the arrow for the moving case). The stationary load (shown on the left) has a relatively plate bending response near the stringer (the vertical member near the left of each plot). Notice that this strong bending response near the stringer is not as prominent, but the response on the leading side of the load is stronger (shown on the right). As observed for the simple load method used in earlier work, the plastic damage on the trailing side of the load compromises the ability of that structure to respond in bending, thereby lowering the overall capacity of the structure.

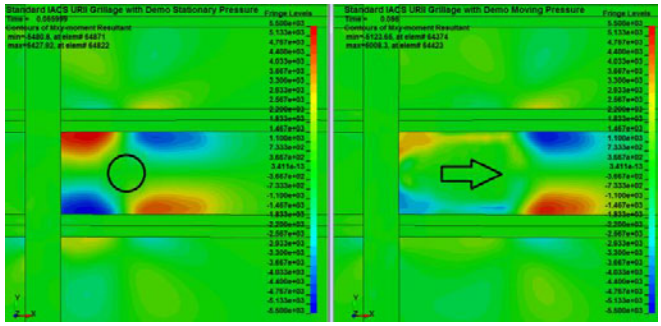

Figure 11. Plot of *Mxy* plate bending near a stringer for a 15 MPa (peak) stationary load (left) and its equivalent moving load (right).

For the central load cases, the bending response to the stationary load is symmetric because the grillage is essentially symmetric about its longitudinal and lateral axes. As with prior observations for the simple load model, the bending response on the trailing side of the moving load is compromised, and is larger on the leading side. This is illustrated for the crushable foam model loads in Figure 12.

The results for the high level load cases are similar but bending plays less of a role because membrane forces in the plate tend to dominate.

Frame Buckling

As previously observed for the simplified load method, frames were observed to be more likely to buckle when subject to moving loads than for stationary loads.

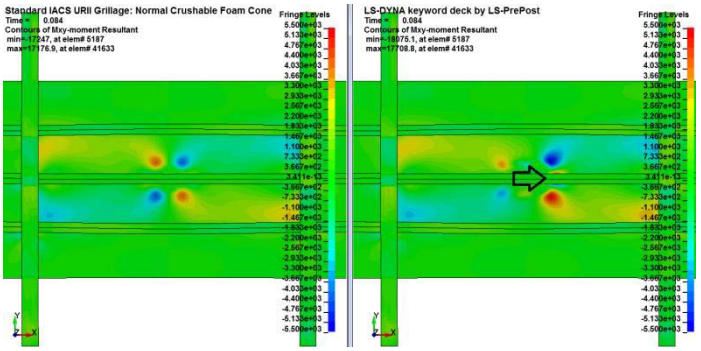

Figure 12. Plot of *Mxy* plate bending at the centre of the grillage for a crushable foam model 25 tonne stationary load (left) and moving load (right).

For all crushable foam model cases near the stringer, stiffener buckling began at roughly the same load level for both the stationary and moving loads; however shortly thereafter, their structural reaction force curves diverged; with the structural reaction force for the moving load case being considerably less than for stationary load case (see Figure 13 as a representative example). This lower reaction force is due to the more severe web frame buckling (in both lateral and longitudinal extent) for the moving load. It should also be noted that in the case of the 25 tonne load on the central frame, there was very little buckling at all compared with the extent of buckling present for the moving case.

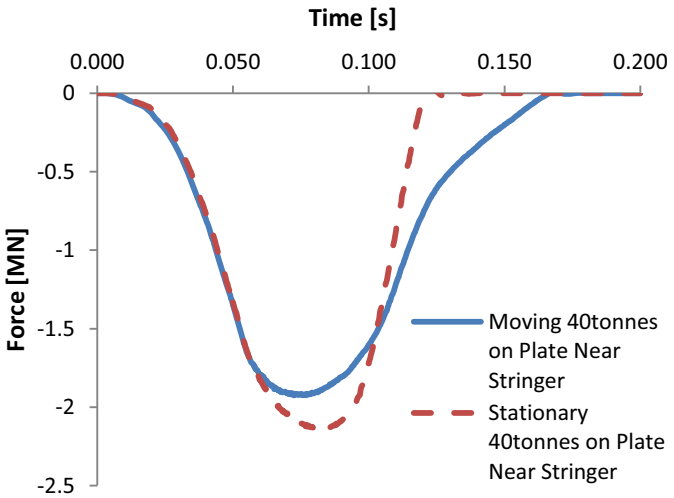

Figure 13. Load history results for the 40 tonne moving and stationary crushable foam load cases acting on the plate between frames near a stringer.

Similar results were observed for the central 40 tonne load cases. No buckling was observed for the 25 tonne load cases.

The 15 MPa (peak) 4D ice pressure method loads were not high enough to cause frame buckling in any case, and even the 30 MPa (peak) pressures did not cause stiffener buckling for the central load cases. The 30 MPa (peak) load cases did cause stiffener buckling for the near stringer load cases. Again, the buckling induced by the moving load was far greater than for the stationary (see Figure 14).

Extent of Deformation and Plastic Damage

The extent of residual plastic damage was consistently found to be greater for the moving load cases than for the stationary load cases; despite loading model. These results are consistent with previous observations made using the simple load model. Figure 15 and Figure 16 show the effective residual plastic strain for a near stringer 15 MPa (peak) 4D ice pressure method load case, and a 25 tonne central crushable foam method load case, respectively.

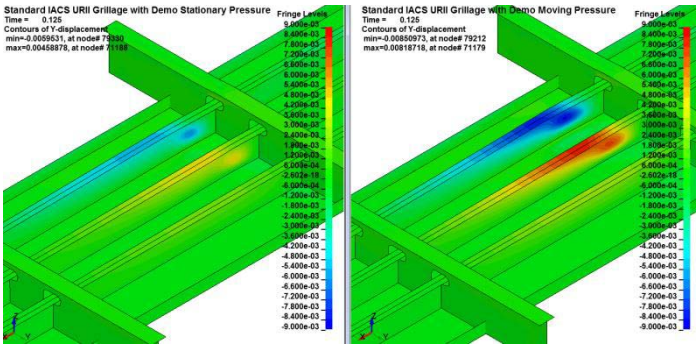

Figure 14. Buckling displacement plot for 30 MPa (peak) 4D ice pressure method stationary load (left) and moving load (right).

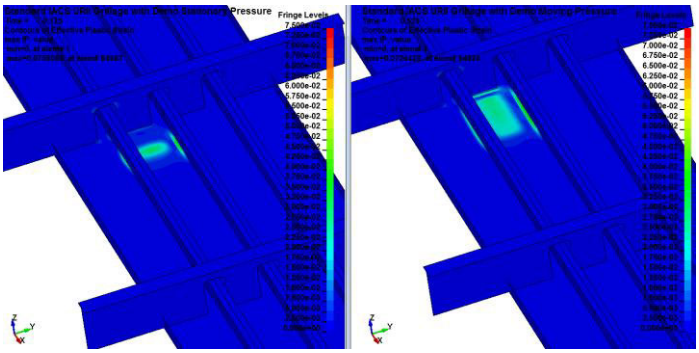

Figure 15. Equivalent plastic strain plot for a 15 MPa (peak) 4D pressure method stationary load (left) and moving load (right).

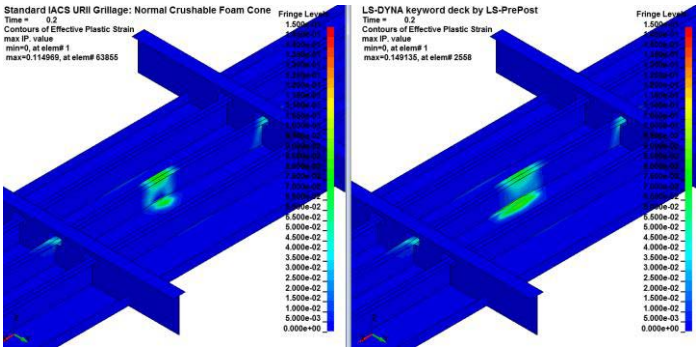

Figure 16. Equivalent plastic strain plot for a 25 tonne crushable foam method stationary load (left) and moving load (right).

CONCLUSIONS

Prior work by the authors questioned whether or not the analysis and design of ice strengthened structures based on stationary loads was valid when the loads may not be stationary. That work suggested that the structural response mechanisms were indeed different for moving loads, and that treating moving loads as stationary loads may not provide the level of conservatism necessary for structural analysis and design. That work was an initial investigation that necessarily made use of an overly simplistic load model in which the normal and tangential motions of a moving load were decoupled, and the load was provided by a rigid indenter.

The present work has attempted to address the shortcomings of the previous work by employing two realistic ice load models that provide adequate pressure distributions and ice motions. Results from simulations using these realistic models agree with the findings of the previous work. That is, moving loads cause substantially more damage than stationary loads, and therefore, structures do not have the same capacity to withstand moving loads as they do stationary loads.

Plastic limit states design is increasingly being employed for ships and offshore structures. The limit states themselves will change depending on whether the load is moving or stationary. The effect of moving loads must be considered, especially for a first-principles design.

ACKNOWLEDGEMENTS

This work was made possible through funds provided by the Memorial University of Newfoundland's Sustainable Technology for Polar Ships & Structures (STePS^2) project and its funding partners.

REFERENCES

Daley, C. G., and G. Hermanski. 2008a. *Ship frame research program - an experimental study of ship frames and grillages subjected to patch loads, volume 1 - data report.* Ship Structure Committee, SSC Project SR 1442 - Final Report; OERC Report 2008-001; NRC-IOT Report TR-2008-11.

———. 2008b. *Ship frame research program - an experimental study of ship frames and grillages subjected to patch loads, volume 2 - theory and analysis reports.* Ship Structure Committee, SSC Project SR 1442 - Final Report; OERC Report 2008-001; NRC-IOT Report TR-2008-11.

Gagnon, R. E. 2004a. Analysis of laboratory growler impact tests. *Cold Regions Science and Technology* 39 (1).

———. 2004b. Physical model experiments to assess the hydrodynamic interaction between floating glacial ice masses and a transiting tanker. *Journal of Offshore Mechanics and Arctic Engineering* 126 (4) (November).

———. 2004c. Side-viewing high-speed video observations of ice crushing. *Proceedings of IAHR 2004*, vol. 2. St. Petersburg, Russia (2004), pp. 289–298

Gagnon, R. E. 2007. Results of numerical simulations of growler impact tests. *Cold Regions Science and Technology* 49 (3) (9).

Gagnon, Robert, David Cumming, Ron Ritch, Robin Browne, Michelle Johnston, Robert Frederking, Richard McKenna, and Freeman Ralph. 2008. Overview accompaniment for papers on the bergy bit impact trials. *Cold Regions Science and Technology* 52 (1) (3).

IACS. 2007. *Requirements concerning polar class*. London: International Association of Classification Societies.

Kendrick, A., C. G. Daley, and B. W. Quinton. 2009. Scenario-based assessment of risks to ice class ships. Paper presented at Offshore Technology Conference 2009, Houston, Texas, USA.

Paik, J. K. 2007. Practical techniques for finite element modeling to simulate structural crashworthiness in ship collisions and grounding (part I: Theory). *Ship and Offshore Structures* 2 (1).

Quinton, B. W. 2009. Progressive damage to a Ship's structure due to ice loading. Masters, Memorial University of Newfoundland.

Quinton, B. W., C. G. Daley, and R. E. Gagnon. 2010. Effect of moving ice loads on the plastic capacity of a ship's structure. Paper presented at Proceedings of the 9th International Conference and Exhibition on Performance of Ships and Structures in Ice, Anchorage, Alaska, USA.

St. John, J., C. Daley and H. Blount, 1984. *Ice Loads and Ship Response to Ice*. Interagency Ship Structure Committee, Rpt no. SSC-329, Washington, DC.